The Human-Height Measurement Scheme Using Image Processing Techniques

Wen-Yuan Chen * and Chih-Hung Wang

Abstract

For human height measurement; there are have contact and non-contact techniques. In this paper, we use a fixed laser point and triangular distance measurement method to construct a non-contact measurement scheme. In hardware, a laser beam was used for signal emission, and a digital camera was used as the signal detection. In software, the distance between the laser beam projection image and the center of the image was used to get the measured length. On the other hand, an offset compensation data was used to calibrate the error and increase the measurement precision. The furthermore, we adjust the space d between the laser and digital camera to get a better measurement precision. All kinds of various conditions were used to simulation. The experimental results reveal our proposed scheme has two advantages when it compares with other method: one is our method can achieve a non-contact human height measurement securely. The other is our scheme is very precise and simple. We simply use a laser pointer and a camera associated with image detection techniques to obtain a precise human height measurement.

Keywords: human height measurement, triangular principle, non-contact measurement, image detection.

1. Introduction

Nowadays, non-contact distance measurement becomes a very popular method. Claudio et.al [1] presented TOF (time-of-flight) ultrasonic distance measurement method. It calculates the time of the ultrasonic wave to and from the object to get distance. However, the accuracy of the distance calculation is not enough for the TOF method. Especially, the ultrasonic wave is shorter. In order to rescue this drawback, Matar et.al [2] proposed a phase difference calculating method by means of ultrasonic wave. However, the accuracy varies depending on the object distance of this method. It is better on near distance. But, it is not good for long distance measurement. In the scheme, the more incline angular of the object is bigger, the more scatter reflection is diverting.

Palojarvi et. al [3] present a laser pulse for distance measurement. In his scheme, a laser pulse was used for signal emission then they calculate the arrival and departure time of the signal to convert the distance. This method makes measurement easily, but worse accuracy. However, it gets the system rapidly suited for military applications. Eugene [4] published an interference laser measurement technique. He used two coherent laser beams to generate interference picture. By means of their different phase caused by distance traveled to computer the distance. It analyzes the interference stripe to obtain the laser beam path differently. Since the air disturbance affects the measurement results, the interference laser measurement just only suitable for stable environment. Beside, the surface and reference of the tested object need to have the high flattening and reflection thus it is suited for indoor measurement and limited in a hundred meters. Poujouly and Journet [5] presented a phase shift laser distance measurement. It calculates the phase shift of the transmitted and received modulated laser waves to get the distance. It has a high precise measurement advantage but this driven circuit is very complicated.

Ens and Lawerence [6] checked filter table and pre-computed one by one to find out the suitable filter. Next, the filter ferrets out the corresponding depth of field. Experiences result shows that it is more precise to the reverse filter method.

Rajagopalan and Chaudhuri [7] divided the image into many sub-images and superimposed the sub-images by using block shift variant blur model. It solves the superimposing problem caused by PSF image in neighbor blocks.

Grosso and Tistarelli [8] proposed a binocular vision image technique to get the depth of field. Illingworth and Hilton [9] used several CCD cameras to catch multi-vision points. They adopt similar features and geometry projective to compute the shape and distance of the object. However, the similar points must be accurate and it is hard to identify. The drawbacks of using CCD image processing are a great quantity data need to be processed, the algorithm was complicated, and it was time- consuming.

*Corresponding Author: Wen-Yuan Chen
(E-mail: cwy@ncut.edu.tw)
[1] Department of Electronic Engineering,National Chin-Yi University of Technology, Taichung, Taiwan, R.O.C. No.57, Sec. 2, Zhongshan Rd., Taiping Dist., Taichung 41170, Taiwan (R.O.C.)

Buerkle and Fatikow [10] presented a triangular principle distance measurement method. It emitted a laser beam and calculates the laser point variation of the object to get the distance. It is a kind of image processing techniques. However, its mechanism is simple, but precise is not good enough.

Rioux et. al.[11] use the refraction principle of multiple optical lens to develop a distance measurement method. First, the laser beam was emitted by semi-conductor, and the CCD camera received the reflection wave from the object. Since the CCD camera and reflect lens are fixed, the mechanism is more complicated, and the size is bigger. Besides, the rotation range of reflection lens is proportional to the space.

Sasaki et. al [12] let CCD camera and 2D laser pictures in synchronize to complete speed computation, and simplified the mechanism. However, it is easily influenced by lens amplify times therefore it precise range is within 10 cm. Some other measurement techniques by image processing techniques can be found in [13-15].

In this paper, we use the triangular principle method, a fixed camera, a laser pointer and the image detection techniques to achieve a human height measurement. The remainder of this paper is organized as follows: Section 2 gives a presentation of the measurement principle. Section 3 illustrates the algorithm of the human height measurement. Section 4 presents the algorithm's experimental results. Section 5 is the conclusion of this paper.

2. Measurement Principle

2.1 Triangular Distance Measurements Technique

For a non-contact distance measurement, we use a laser point and triangular distance measurement technique to achieve the goal. Figure 1 shows the diagrammatic sketch of the triangular measurements principle. The camera and the laser are faced to the object, and settled on parallel. In system operation, the laser pointer emits a laser beam to the object. The camera receives the laser point projection location in the image. Due to the laser beam to the object is parallel to the center of the principal axis of the camera, thus the distance can easily get by calculating trigonometric functions. The laser beam is shown by a high-light projection in the image. Because the projection is fixed and explicit, thus the object distance can get by calculating the distance between the projection along the x-axis and image center. However, the object distance is farther when the laser projection is more close to the image center.

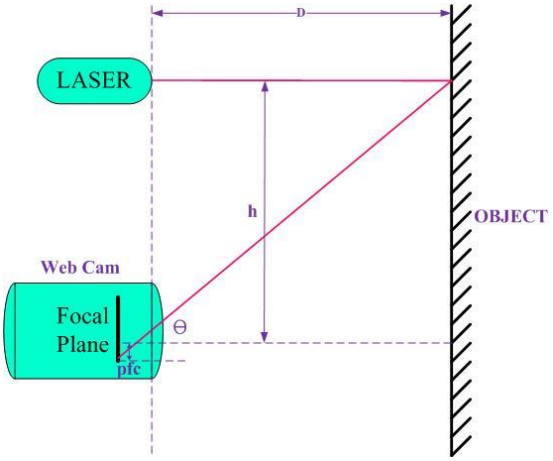

Figure 1: The diagrammatic sketch of the triangular measurements principle.

As figure 1 display, D is the object distance; h express the space between the center of focal plane and laser. The angular between the laser projection and the center of focal plane is θ . Then, the distance can be calculated by the following formulas and listed it below:

$$D = \frac{h}{tan\theta} \tag{1}$$

$$\theta = pfc * rpc + ro \tag{2}$$

Where ***rpc*** express the arc of the pixel, ***pfc*** are the pixels from the laser projection to the center of focal plane, and ***ro*** is the compensation of the arc.

Replace (2) into (1), we get equation (3).

$$D = \frac{h}{tan(pfc * rpc + ro)} \tag{3}$$

From the mathematical, we easily obtain ***pfc*** by counting the pixels between the center of the focal plane and laser projection point in the image. Next, we use the parameter ***ro*** and ***rpc*** to compensates the align error; both parameters are get from several times calibration. After simulations, we correct the system by adjusting the parameters. Finally we calculate the angular by using equation (4).

$$\theta_{actual} = arctan\left(\frac{h}{D_{actual}}\right) \tag{4}$$

Where θ_{actual} denote the true angular, and D_{actual} is measured distance. Following this rule, we can compute the distance of an object easily. However, the system reveals a drawback; the precisions vary on different distances in practical.

2.2 Improving the Measurement Precision

Since the different distance of the pixel and principal axis cause the different side direction amplifier, it will induce the capture image distortion. Therefore, some compensation is needed to calibrate the error in distances calculation by means of camera and image techniques. In this paper, we adopt the piecewise linear concept associate with the bi-linear interpolation method to adjust the nonlinear problem. We divide the distance to be measured into several pieces. And then a compensation table is created to record the authentic values use as each calibration points. In practice, we set the space of the calibration piece as 5 cm under 640x480 image resolution at 12.7 cm space between laser and camera as figure 2 shown. Table 1 is the calibration table; its measured ranges are from 35 cm to 220 cm. It includes the parameters such as item, real distance, X-axis, pixels between X-axis and the center of image under Y-axis is 240.

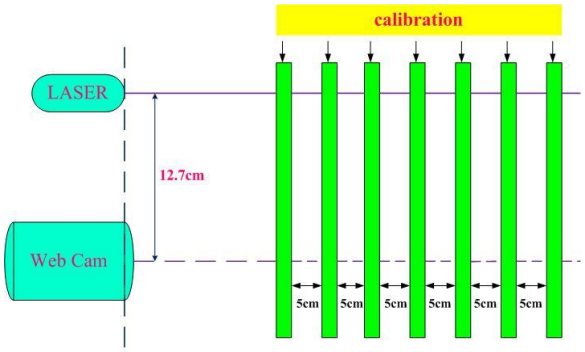

Figure 2: The diagrammatic sketch of the measurement distances calibrates concept.

Table 1: The calibration table under Y-axis is 240 and the pixel is 0 between Y-axis and the center of image.

item	Real distance	X-coordinate	Y-coordinate	X-distance	Y-distance
1	35	20	240	300	0
2	40	53	240	267	0
3	45	80	240	240	0
4	50	101	240	219	0
5	55	119	240	201	0
6	60	134	240	186	0
7	65	146	240	174	0
8	70	159	240	161	0
9	75	166	240	154	0
10	80	174	240	146	0
11	85	181	240	139	0
12	90	187	240	133	0
13	95	193	240	127	0
14	100	198	240	122	0
15	105	203	240	117	0
16	110	207	240	113	0
17	115	211	240	109	0
18	120	214	240	106	0
19	125	217	240	103	0
20	130	220	240	100	0
21	135	223	240	97	0
22	140	226	240	94	0
23	145	229	240	91	0
24	150	231	240	89	0
25	155	233	240	87	0
26	160	235	240	85	0
27	165	236	240	84	0
28	170	238	240	82	0
29	175	240	240	80	0
30	180	242	240	78	0
31	185	243	240	77	0
32	190	244	240	76	0
33	195	246	240	74	0
34	200	247	240	73	0
35	205	248	240	72	0
36	210	249	240	71	0
37	215	250	240	70	0
38	220	251	240	69	0

Lookup table is a quick and effective method for calibrating the errors caused by lens distortion. Since the laser beam is parallel to the camera, so that the high-light laser point always locates on the same horizontal line. This phenomenon makes the pixels between the Y-axis and the center of the image equal to zero. It makes the Y coordination fixed. According to the table 1, the Y coordination is 240. In our structure, the pixels vary depending on the object distance. Simultaneously, the more leaser point is close to the center of the image, the pixels become lesser. It means the distance of the object is more far from the camera. On the contrary, when the laser point is far from the center of the image, the pixels become more. It shows that the distance of the object is near to the camera. In practical measurement, we calculate the pixels between the X-axis and the center of the image. And then the compensation is made by look up the calibration table to get a more correct measure value. Finally, we get the distance measurement by using equations (5-6) and the substitution method.

Fig. 3 shows the distances measurement calibration flow chart. Where the distances of the test object is D_r and it position falls in calibration points A and B. D_a and D_b denote the distance of the point A and B respectively. Three notations P_r, P_a, and P_b express the pixels count from the center of the image to reflection points of the above three points mapping to the image. By using the piecewise linear method, we can calibration the error by calculating equation (5) and (6) listed below.

$$D_r = \frac{D_b - D_a}{P_a - P_b} \times (P_a - P_r) + D_a \qquad (5)$$

From lookup table, we get $D_b - D_a = 5cm$ substitute it to (5) and obtain

$$D_r = \frac{P_a - P_r}{P_a - P_b} \times 5 + D_a \qquad (6)$$

Where D_r is the desired distance of the test object. It is more precise compared with before compensation operation.

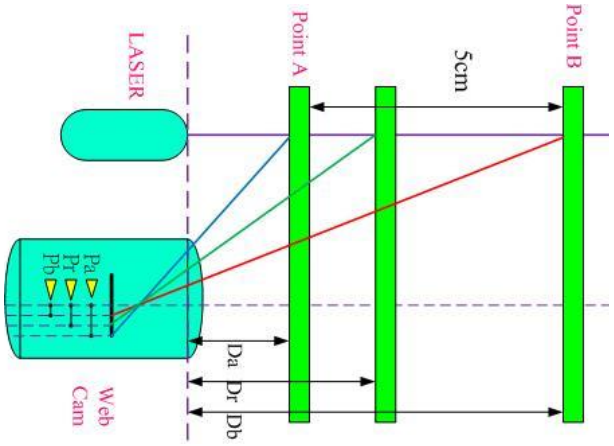

Figure 3: The diagrammatic sketch of the measurement distances calibration by using camera and image processing techniques

3. Human Height Measurement Algorithm

In the system design, a red point image that laser beam projects at the object use to calculate distance by image processing techniques. The main flow of human height measurement is shown in Figure 4. Before the system start, we set the camera to capture the image. Then the region of interesting (ROI) stage is used to confine the candidate region for further processing. The red color area capture (RCAC) stage grasp the red color area because it is the detect target. Successively, the color image into binary image (C2B) is used for simplifying the detection procedure. Besides, the topologic filtering (TF) stage is used to filtering the image noise and center of gravity detection (CGD) stage make sure the laser beam projection point. Finally, the target point is got, and the triangular measurement method (TMM) stage computes the distance of the measure object and sent the results output. The relative operation are described in the following.

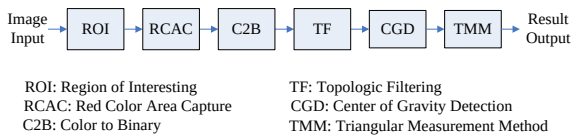

Figure 4: The image detection flow chart of the human height.

3.1 Region of Interesting and Red Color Area Capture

In hardware structure, we set the laser pointer in the left side of the camera and mount them in parallel state of the mechanism. Figure 5 shows the schematic diagram of the measure machine. It is important that the orientation of the laser beam and camera caption orientation is coincided. This makes sure the laser beam projection red point can appearing in a fixed range in the image captured by the camera. For this reason, the laser project point area can be just selected to minimize the image processing time. Therefore, we select the range coordinate X from 0-320, coordinate Y from 0-320 of the image as the ROI. Figure 8(a) shows the human height measurement case and figure 8(b) shows the corresponding ROI area. Because the ROI manipulation, the system can speed up 48 times.

Table 2 shows the optical spectrum of the visible light. We see the wave length of the laser beam is at the range 622-780 nm. From the table 2, it is in accordance with red color in RGB color planes. Intuitively, we use red color detection to grasp the red point of the laser beam project. For eliminating the noise interference, we select the biggest red area as the target. After necessary image processing, the ROI and red color detection is achieved, and the results are shown in figure 6.

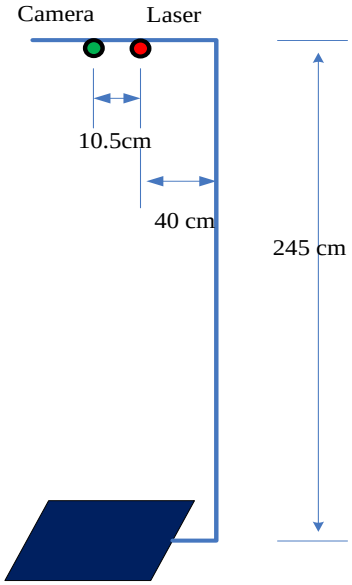

Figure 5: The schematic diagram of the human height measurement machine.

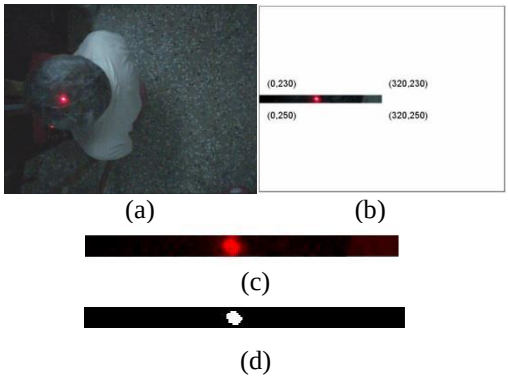

Figure 6: The image preprocessing; (a) the input image, (b) the image of ROI, (c) The extracted color areas, (d) the binary

image of (c), (e) the image after topologic filter of (d).

3.2 Colors to Binary Mapping and Topologic Filtering

A: Colors to Binary Mapping

Due to the binary plane is more suitable than color planes thus; a color to binary mapping is used in our method. Usually, a color image is represented by RGB planes. Therefore, we use the red laser pointer for signal emitter. Since the R-plane has 256 gray scales, thus a threshold value is used to divide the R-plane into two levels. In this article, we set the threshold value=128 to map the R-plane into the binary plane. The test image is shown in Figure 6, and figure 6(d) shows the binary image after figure 6(c) is binary mapped. From the simulation results, it reveals that the C2B method is an effective method.

Table 2: The optical spectrum of the visible light

Color	Range of frequency (THz)	Wave length (nm)
Red	384-482	622-780
Orange	482-503	597-622
Yellow	503-520	577-597
Green	520-610	492-577
Blue	610-659	455-492
purple	659-769	390-455

B: Topologic Filtering

For reducing processing time, we select a ROI area to decrease the image size. Besides, we use the red color area detection and binarization stage to obtain the laser projection point as Figure 6(c) shows. Figure 6(d) shows the detected target area in binary plane. However, figure 6(d) shows some noises existed. It turns black point into white points, and white points into black points. In order to eliminate the noise, we use a topologic filter to accomplish the goal. In this method, the notation A is used to express the binary image and B is the 3*3 square masks. The notation AΘB stand for the erosion operation and A $\oplus$ B delegate the dilation operation. Finally, the opening operation (A $\circ$ B) and closing operation (A˙B) are adopted to filter out the noise.

3.3 Center of Gravity Detection

The laser beam project to the image forms a small circle with some pixels, thus a coordinate (X,Y) used to record the laser projection point. Intuitively, the center of gravity of object is an appropriate to denote the object. In this article, we use the idea of the center of gravity to calculate the coordinate of the laser beam projection in image. The equation used to calculate the center of gravity is describing below:

$$(X,Y)=\left(\frac{1}{n}\sum x,\frac{1}{n}\sum y\right) \quad (7)$$

Where, X and Y is the coordinate X-axis and Y-axis of the center of gravity respectively. The n denote the total pixels of the laser point.

3.4 Distance Calibration

In order to obtain human-height measurement, we used the Eqs. (1-7) to achieve the goal. However, use compensation for improving the precision is necessary. In intuitively, the bi-linear interpolation technique was used to minimize the measurement error is suitable. Figure 7 shows the calibration concept. The vertical ruler is used to calculate the compensate measurement error. In practical, we use each 5 cm as a calibration point for measure values within the range.

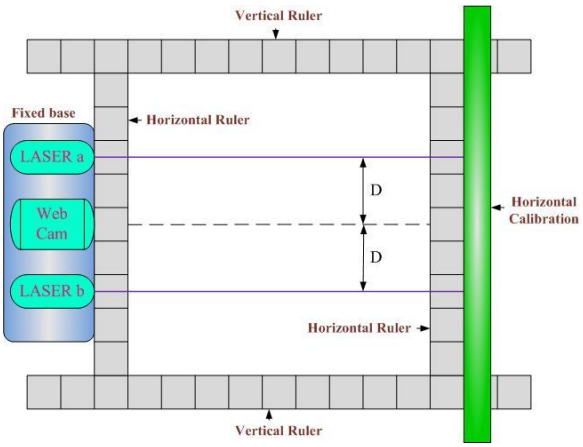

Figure 7: Calibration concept.

4. Experiment Results

4.1 Experiment Environmental

In simulation, several devices are adopted to construct the scheme. We use the laser pointer with wave length in the range 630 ~ 670nm, it is belonging to the color red wave length at measurement. At the same time, we use two types' cameras for test; one is the low resolution camera QuickCam web-camera. It with the resolution size is 640*480, which is produced by Logitch Company. Another type is the high resolution camera Nikon S600 with size 3648x2736, which is produced by Nikon Company. For analyzing the accuracy, there are two kinds distance between the laser and camera to simulate on the experience. In practical, we use 10.5 cm and 32.7cm for the short distance and long distance measurement, respectively. Besides, we use the 12.7 cm distance for short distance measure which is below 150 cm under web-camera. Figure 8 shows the facility and devices of the human height measure system. Figure 8(a) displays the major

facility computer and camera. Figure8(b) shows the space between the laser and web-camera.

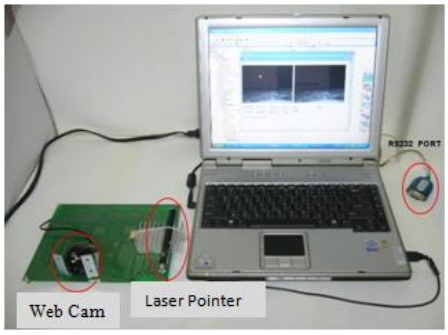

(a)

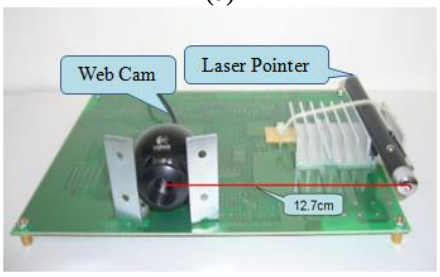

(b)

Figure 8: The facility and devices of the human height measure system; (a) human height measure facility, (b) the laser and web-camera on the board.

4.2 Measurement results

Figure 9 is the human height measurement mechanism. Figure 9(a) shows the detection device and Figure 9(b) shows the man measurement operation. Figure 10 shows the laser point was used to measure the human height. Figure 10(a) is the test image, and Figure 10(b) displays the measure results at the distance and human height value which is corresponding to figure 10(a).

We use two type cameras in the simulation. The low resolution camera QuickCam web-camera is suitable for below 150 cm measuring case. In high resolution measurement, we use the camera, Nikon S600 for simulation. We set two situations: one is the short space between laser and camera is 10.7 cm, it is suitable for near object distance measurement. Another is the long space between laser and camera is 32.7 cm, it is good for far object distance measurement. Table 3 shows the calibration table under the space between laser and camera is 10.7 cm for Nikon S600 digital camera. Table 4 show the measure results, it is suitable for measuring the human height below 180 cm. And it is under using Table 3 as the calibration tables, and its maximum measurement distance is 220 cm. On the other hand, we use Table 5 as the calibration table when the space between laser and camera is 32.7 cm for Nikon S600 digital camera. Table 6 shows the measure results, it is suitable for the human being height below 240 cm. And it adopts Table 5 as the calibration table, It can measure the maximum distance is 245 cm. From the simulation results, we can find that the more space between laser and camera is far, the more accuracy is better.

(a) (b)

Figure 9: The human height measurement mechanism; (a) the detection device, (b) The man measurement operation

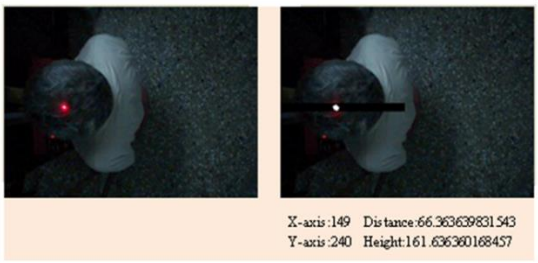

Figure 10: the red point was used to measure the human height; (a) the red point on the test image, (b) the measure results at the distance and human height value.

Table 3: The calibration table used in the 10.7 cm distances between laser and camera for Nikon S600 digital camera.

item	Real distance	X-coordinate	Y-coordinate	X-distance	Y-distance
1	20	281	1372	1543	-4
2	25	570	1374	1254	-6
3	30	756	1375	1068	-7
4	35	893	1375	931	-7
5	40	1003	1377	821	-6
6	45	1087	1378	737	-10
7	50	1153	1379	671	-11
8	55	1207	1379	617	-11
9	60	1255	1380	569	-12
10	65	1293	1380	531	-12
11	70	1328	1380	496	-12
12	75	1356	1381	468	-13
13	80	1383	1381	441	-13
14	85	1406	1382	418	-14
15	90	1426	1382	398	-14
16	95	1445	1382	379	-14
17	100	1450	1382	364	-14
18	105	1475	1383	349	-15
19	110	1488	1383	336	-15
20	115	1501	1383	323	-15
21	120	1513	1383	311	-15
22	125	1523	1383	301	-15
23	130	1533	1383	291	-15
24	135	1542	1383	282	-15
25	140	1550	1383	274	-15
26	145	1557	1383	267	-15
27	150	1565	1383	259	-15
28	155	1571	1383	253	-15
29	160	1577	1384	247	-16
30	165	1583	1384	241	-16
31	170	1589	1384	235	-16
32	175	1595	1384	229	-16

33	180	1600	1384	224	-16
34	185	1604	1384	220	-16
35	190	1608	1384	216	-16
36	195	1612	1384	212	-16
37	200	1616	1384	208	-16
38	205	1620	1384	204	-16

Table 4: The measurement results listed in the 10.7 cm distances between laser and camera.

Item	Real distance	Relative Distance	Measurement distance
1	27	1174	27.15
2	37	884	37.14
3	47	713	46.82
4	57	599	57.09
5	67	518	66.86
6	77	458	76.85
7	97	411	86.75
8	97	374	96.67
9	107	345	106.54
10	117	319	116.67
11	127	298	126.5
12	137	280	136.25
13	147	265	146.23
14	157	252	155.83
15	167	240	165.83

(a)

Item	Real height	Measured height	Error
1	193	192.85	-0.15
2	183	182.86	-0.14
3	173	173.18	0.18
4	163	162.91	-0.09
5	153	153.14	0.14
6	143	143.15	0.15
7	133	133.25	0.25
8	123	123.33	0.33
9	113	113.46	0.46
10	103	103.33	0.33
11	93	93.5	0.50
12	83	83.75	0.75
13	73	73.57	0.57
14	63	64.17	1.17
15	53	54.17	1.17

(b)

Table 5: The calibration table used in the 32.7 cm distances between laser and camera for Nikon S600 digital camera.

Item	Real Distance	x-coordinate	y-coordinate	X-distance	Y-distance
1	55	48	1371	1776	-3
2	60	183	1372	1641	-4
3	65	300	1374	1524	-6
4	70	395	1374	1429	-6
5	75	485	1375	1339	-7
6	80	561	1376	1263	-8
7	85	628	1377	1196	-9
8	90	690	1378	1134	-10
9	95	745	1378	1079	-10
10	100	795	1379	1029	-11
11	105	839	1379	985	-11
12	110	880	1380	944	-12
13	115	918	1381	906	-13
14	120	953	1381	871	-13
15	125	985	1381	839	-13
16	130	1014	1382	810	-14
17	135	1041	1381	783	-13
18	140	1066	1382	758	-14
19	145	1090	1383	734	-15
20	150	1112	1383	712	-15
21	155	1133	1382	691	-14
22	160	1152	1383	672	-15
23	165	1172	1381	652	-13
24	170	1189	1383	635	-15
25	175	1205	1383	619	-15
26	180	1220	1383	604	-15
27	185	1235	1384	589	-16
28	190	1249	1384	575	-16
29	195	1262	1384	562	-16
30	200	1274	1384	550	-16
31	205	1288	1383	536	-15
32	210	1299	1383	525	-15
33	215	1310	1383	514	-15
34	220	1319	1383	505	-15
35	225	1328	1383	496	-15
36	230	1336	1384	488	-16
37	235	1345	1385	479	-17
38	240	1353	1384	471	-16

Table 6: The measurement results listed in the 32.7 cm distances between laser and camera.

Item	Real distance	Relative Distance	Measurement distance
1	57	1719	57.11
2	67	1484	67.11
3	77	1310	76.91
4	87	1172	86.94
5	97	1061	96.8
6	107	970	106.83
7	117	891	117.14
8	127	828	126.9
9	137	773	137
10	147	726	146.82
11	157	684	156.84
12	167	646	166.76
13	177	614	176.67
14	187	584	186.79
15	197	558	196.67

(a)

Item	Real height (cm)	Measured people height	errror (cm)
1	188	187.89	-0.11
2	178	177.89	-0.11
3	168	168.09	0.09
4	158	158.06	0.06
5	148	148.2	0.20
6	138	138.17	0.17
7	128	127.86	-0.14
8	118	118.1	0.10
9	108	108	0.00
10	98	98.18	0.18
11	88	88.16	0.16
12	78	78.24	0.24
13	68	68.33	0.33
14	58	58.21	0.21

15	48	48.33	0.33

(b)

4.3 Compare with other methods

There are many papers are study on the human measurement, therefore, we make a comparison with other methods. Table 7 shows the features comparison table among other's methods and proposed methods. The contacted measure method is a traditional method; it usually includes a mechanism structure. The advantage of the traditional method has low complexity, low response, low safety, and low measure speed. For proposed method compared with Matar's method [2], they are all non-contact measurement system with high safety, high measure response, and high measure speed. Besides, the proposed method with low complexity circuit design and high resolution advantages is superior than other's method.

Table 7: The features comparison among Other's method and proposed method

order	item	Contacted method	Matar's Method [2]	Proposed method
1	Contact object	Yes	No	No
2	Safety	low	high	high
3	Type	Mechanism	ultrasonic wave	Image detection
4	Response	low	high	high
5	Resolution	low	medium	high
6	Complexity	low	high	low
7	Measure speed	low	high	high

5. Conclusions

In human height measurement, there are several methods it includes contact and non-contact measurement. In this study; we use triangular measure principle to develop a human height non-contact measurement. In the structure, a laser beam was used for signal emission and digital camera was used as the signal detection. Besides, a data calibration stage was used to improve the measurement precision. For demonstrating the effectiveness and correctness of the proposed scheme, simulations under all kinds of various conditions were conducted. Simulation results show that when the distance between the laser and digital camera is shorter, then the measurement height is shorter. On the contrary, when the distance between the laser and digital camera is longer, then the measurement height is taller.

References

[1]. C. Claudio, C.D. Giorgio, M. Brouno, P. Maria, and T. Andrea, "A temperature compensated ultrasonic sensor operating in air for distance and proximity measurements", IEEE Transactions on Industrial Electronics, Vol.IE-29,No.4,pp. 336-341, Nov. 1982.

[2]. O.B. Mater, J.P. Remenieras, C. Bruneel and A. Roncin, F. Patat, "Noncontact measurement of vibration using airborne ultrasound", IEEE Transactions on Ultrasonics, Ferroelectrics and Frequency Control, Vol.45, No.3, pp. 626-633, May 1998.

[3]. P. Palojarvi, K. Maatta and J. Kostamovaara, "Integrated Time-of-Flight Laser Radar", IEEE Transactions on Instrumentation and Measurement, Vol. 46, No.4 , pp. 996 -999, Aug 1997.

[4]. Eugene Hecht, "Optics", 3rd edition, Addison Wesley Longman, 1998.

[5]. S. Poujouly and B. Journet, "A twofold modulation frequency laser range finder", J. Opt. A: Pure Appl. Opt., Vol. 4, pp. 356-363, 2002.

[6]. J. Ens and P. Lawrence, "An Investigation of Methods for Determining Depth from Focus", IEEE Trans. PAMI, Vol.15, No.2, pp. 97-108, Feb 1993.

[7]. A.N. Rajagopalan and S. Chaudhuri, "A Block Shift-Variant Blur Model for Recovering Depth From Defocused Images", Image Processing, Proceedings, International Conference on, Vol.3, pp.636-639, Oct 1995.

[8]. E. Grosso and M. Tistarelli, "Active Dynamic Stereo Vision", IEEE Trans. on pattern analysis and machine intelligence, Vol. 17, No.9, pp. 868-879, Sep 1995.

[9]. J. Illingworth and A. Hilton, "Automatic construction of static object models using computer vision", Electronics & Communication Engineering Journal, Vol.10, Issue.3, pp.103-113, June 1998.

[10]. A. Buerkle and S. Fatikow, "Laser Measuring System For a Flexible Micromanipulation Station", Proceedings of 2000 IEEE/RSJ International Conference On Intelligent Robots And Systems, pp. 799-804, 2000.

[11]. M. Rioux, F. Blais, J. Beraldin and P. Boulanger, "Range imaging sensors development at NRC Laboratories", Interpretation of 3D Scenes, pp.154-160,1989.

[12]. K. Sasaki, N. Ishikawa, T. Otsuka and M.

Nakajima, "3D image location surveillance system for the automotive rear-view", Vehicle Navigation and Information Systems Conference Proceedings, pp. 27-32, 1994.
[13]. Chuin-Mu Wang, Tsung-Hung Lin; Ruey-Maw Chen and Sheng-Chih Yang, "Application of Grey System Theory in MRI Classification," Biomedical Engineering : Applications, Basis And Communications Vol. 22, No. 2 pp 111–118, 2010.
[14]. Chuang LY, Yang CH, Jin LC, Classification of multiple cancer types using fuzzy support vector machines and outlier detection methods, Biomed Eng Appl Basis Commun 17(6):300–308, 2005.
[15]. Lee WL, Hsieh KS, Chen YC, Chen YC, A study of ultrasonic liver images classification with artificial neural networks based on fractal geometry and multiresolution analysis, Biomed Eng Appl Basis Commun 16(2):59–67, 2003.

Wen-Yuan Chen was born in Taichung, Taiwan, in 1957. He received the B.S. and M. S. degrees in Electronic Engineering from National Taiwan University of Science and Technology in 1982 and 1984, respectively, and the Ph.D. degree in Electrical Engineering from National Cheng Kung University in Tainan Taiwan, in 2003. Since 2007, he has been a Professor in the Department of Electronic Engineering at National Chin-Yi University of Technology. His research interests include digital signal processing, image compression, pattern recognition and watermarking.